

**High-fidelity readout scheme for rare-earth solid-state quantum computing**A. Walther,<sup>\*</sup> L. Rippe, Y. Yan,<sup>†</sup> J. Karlsson, D. Serrano, A. N. Nilsson, S. Bengtsson, and S. Kröll*Department of Physics, Lund University, 221 00 Lund, Sweden*

(Received 31 March 2015; published 10 August 2015)

We propose and analyze a high-fidelity readout scheme for a single-instance approach to quantum computing in rare-earth-ion-doped crystals. The scheme is based on using different elements as qubit and readout ions, where the readout ions are doped into the material at a much lower concentration than the qubit ions. It is shown that by allowing the qubit ion sitting closest to a readout ion to act as a readout buffer, the readout error can be reduced by more than an order of magnitude. The scheme is shown to be robust against certain experimental variations, such as varying detection efficiencies, and we use the scheme to predict the attainable quantum fidelity of a controlled NOT (CNOT) gate in these solid-state systems. In addition, we discuss the potential scalability of the protocol to larger qubit systems. The results are based on parameters which we believe are experimentally feasible with current technology and which can be simultaneously realized.

DOI: [10.1103/PhysRevA.92.022319](https://doi.org/10.1103/PhysRevA.92.022319)

PACS number(s): 03.67.Lx, 03.65.Wj, 42.50.Dv

**I. INTRODUCTION**

The possibility of realizing a quantum computer is being investigated using a large variety of different experimental implementations. Currently, the largest entangled qubit systems have been realized in ion traps [1,2] and using linear optics with single photons [3]. There is, however, intrinsic value in investigating solid-state systems, as they are generally regarded as having a higher potential for future scalability to larger systems. For solid-state systems, the best progress has been achieved with superconducting circuits [4] and impurity-doped solids, such as nitrogen-vacancy (NV) centers in diamond [5]. Another impurity-doped system, rare-earth ions in crystals, has demonstrated very good performance in terms of quantum memories [6–8] but has yet to demonstrate reliable two-qubit gates between spin qubits or a realistic route towards larger qubit systems. A major obstacle has been that, so far, only large ensembles of rare-earth ions have been used for gate operations [9,10], and this has been shown to scale poorly [11]. A promising approach to scalability in rare-earth quantum computing (REQC) is to move into the single-instance regime, although this requires detecting single rare-earth ions inside their crystal hosts. Bare detection of single ions was just recently realized [12,13] with certainty, but there has been no clear description of how these detection schemes can be directly used in quantum information processing.

In this paper, we present a readout scheme that, in principle, allows for an arbitrarily high readout fidelity of the quantum state of a single ion inside a macroscopic host. The readout scheme is based on using a special buffer step (indicated in Fig. 1) that can be cycled repeatedly, a scheme that is similar in nature to what has been done previously for multispecies atomic clocks [14]. We show that with such a readout, a full

controlled-NOT (CNOT) gate can be performed in these systems with fidelity of about 99% based on simulations that are supported by what is currently experimentally achievable. We also discuss further scaling towards larger multiqubit systems by showing how chains of single ions can be mapped out, and we find that, including most known error sources as discussed in Sec. IV, entangled states of 10 qubits remaining above 92% fidelity appear feasible, as long as all ions can control each other.

It is interesting to note that at the single-ion level, these impurity-doped systems resembles the trapped-ion systems but with two major differences. The first is the advantage that the ions are trapped by the comparatively large trapping potentials of the crystal bindings. This enables the ions to sit much closer to each other than in ion traps (nanometers instead of microns), which in turns allows the direct electrical dipole interactions between ions to be used as an entangling mechanism. The second difference is the disadvantage that the surrounding environment is not vacuum but a crystal host that can cause additional decoherence effects as well as worsen the single-ion detection possibilities through, e.g., scattering. While the disadvantages may at first appear daunting, it is important to note that one of the main limitations to scalability in ion traps is that the entangling mechanism, the common motional modes, becomes increasingly more complex the more ions that are involved [15]. The direct dipole interactions that can be used in REQC, however, do not suffer from this problem, and we thus expect that once the initial hurdle of establishing single-ion readout is overcome, the scaling to a larger number of qubits will be much more manageable.

This paper is organized as follows: In Sec. II the basic single-instance quantum computing scheme is described together with a discussion of reasonable material parameters. Section III details the readout scheme, and in Sec. IV we go through a full CNOT gate from initialization to readout. Further scalability to larger qubit systems is discussed in Sec. V, followed by a summary of our findings in Sec. VI.

**II. OVERVIEW AND PARAMETER CONSIDERATIONS**

The single-instance scheme is based on using single rare-earth qubit ions, where the qubit levels are suitable

<sup>\*</sup>andreas.walther@fysik.lth.se<sup>†</sup>Present address: College of Physics, Optoelectronics and Energy and Collaborative Innovation Center of Suzhou Nano Science and Technology, Soochow University, Suzhou 215006, China, and Key Lab of Advanced Optical Manufacturing Technologies of Jiangsu Province and Key Lab of Modern Optical Technologies of Education Ministry of China, Soochow University, Suzhou 215006, China.

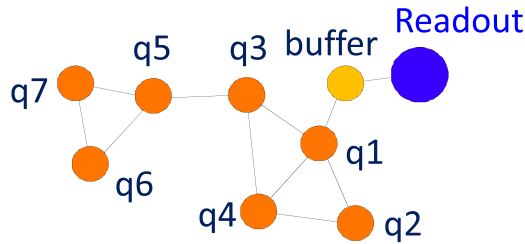


FIG. 1. (Color online) A chain consisting of one readout ion in the vicinity of several qubit ions (e.g., Eu), where the closest qubit ion is being used as a buffer stage (the bright one); see the text for more details. The lines between the ions show which of them can interact directly via frequency shifts caused by changes to the permanent dipole moments. With a 4% doping concentration, it is expected that each Eu ion can, on average, interact with about five other Eu ions surrounding it.

ground-state nuclear-spin states (hyperfine states) with long coherence times and where a long-lived optically excited state can be used for ion-ion interactions. europium has generally demonstrated impressive coherence properties [16], and throughout the paper we will assume Eu as a qubit ion. It is very difficult to detect single ions with long excited-state lifetimes, however, and to circumvent this, several schemes could be considered such as those where a readout ion of a different species is used. Coupling between ions, both between two qubit ions for gates and between a qubit ion and a readout ion for detection, will be mediated via permanent dipole-dipole interactions (dipole blockade effect). In either case, when two ions are sufficiently close, the change in the static dipole moment as one ion is excited is enough to shift the energy level of the neighboring ion out of resonance with a driving laser, thus providing a control mechanism.

Previously, considerable attention has been given to using the short-lived  $5d$  transition in Ce as a potential readout ion [17–19]. However, recent measurements have revealed that Eu absorbs at the same wavelength as the cycling transition in Ce (at least in the favored host material,  $Y_2SiO_5$ ), which makes it necessary to find an alternative readout ion. A very promising scheme for detecting single rare-earth ions is via Purcell enhancement of fluorescence due to coupling of the ion to a high-finesse cavity with a very small mode volume. A fiber-based cavity setup [20] is a suitable candidate and would allow single-ion detection of, in principle, any rare-earth  $4f$  transitions. As an example we will here use Nd, which has a relatively high oscillator strength, but in the case of unexpected energy transfers or overlapping absorption lines, any other rare-earth ion could be used with the same readout scheme with no significant changes.

It will be assumed that we are working with a  $Eu^{3+}:Y_2SiO_5$  crystal, where 4% of the yttrium ions in the crystal host have been replaced with europium, distributed roughly equally in each of two different sites (although with only one isotope). This is a relatively high doping concentration, and simulations have shown that, given the difference between the dipole moment of the ground and excited states, any ion will, on average, have more than five other ions sufficiently close to be controlled by it. It is worth pointing out that it has been shown that the coherence time for Eu is independent of the

doping concentration [21]. For the readout ion, on the other hand, background trace elements of Nd are expected to be enough; no special doping is required since one readout ion is enough for an entire chain of qubits. Eu has an excited-state transition frequency of about 517 THz (580 nm), whereas the qubit nuclear spin levels have splittings on the order of tens of MHz. Also note that while the inhomogeneous width of the ensemble is increased at higher concentrations, the energy splittings of individual ions remain largely unaffected.

Any state-to-state transfer will be done with complex hyperbolic secant (sech) pulses. These chirped pulses have the advantage over simple square pulses that they are robust against certain errors, such as amplitude and frequency fluctuations; see Ref. [22] for more details. Bloch simulations suggest that the Eu ions can be transferred to and from the excited state by such pulses of 400-ns duration with an efficiency of 99.96% (i.e., an error of  $4 \times 10^{-4}$ ), which will be used for the following calculations. The transfer efficiency is limited almost entirely by the duration of the pulse relative to the excited-state lifetime, where the lower limit of the duration is set by the inverse of the qubit nuclear-spin-level separations. It should be noted that the transfer efficiency for Eu has not been fully verified by experiments and does not include effects such as instantaneous spectral diffusion (see, e.g., [23]). It is believed, however, that the effects from spectral diffusion can be strongly mitigated by hole-burning sequences that aim at keeping the total number of ions in the qubit frequency channels very low. The high transfer efficiency can be compared with experiments performed with the similar element praseodymium, where the experimental transfer efficiency matches simulations rather well. For praseodymium, the measured and calculated efficiency is about 96% [10], and the main limitations are the short excited-state lifetime and the limited Rabi frequency available, as well as the fact that an ensemble was used as a qubit. Such an ensemble not only has an inhomogeneous frequency spread but also sits in different spatial parts of the beam profile, making different ions experience different Rabi frequencies. For single-ion Eu transfers inside a cavity, both of those limitations are strongly reduced, and preliminary measurements on Eu ensembles also supports that higher fidelities can be obtained in Eu systems [24].

### III. READOUT SCHEME

The state of the qubit ions can be read out with a readout ion using a permanent dipole blockade mechanism, which is also used for the quantum gates [11,25]. The dipole blockade mechanism is demonstrated in Fig. 2, although for now we will study only a single transfer step, i.e., from the buffer ion (which is a type of qubit ion) to the readout ion. The full scheme of Fig. 2 will be explained later. In order to determine whether one ion is in state  $|0\rangle$  or  $|1\rangle$ , it should be selectively excited to state  $|e\rangle$  with a pulse resonant with the  $|0\rangle \rightarrow |e\rangle$  transition. If the ion is excited, the readout ion's transition frequency is Stark shifted by the dc electric dipole field of the excited state of the qubit ion. This means that a readout laser tuned to the readout ion's unshifted resonant frequency will not excite it.

The readout ion, in our example Nd, has a lifetime of  $100 \mu s$ . With a reasonable cavity finesse of  $10^4$ – $10^5$  and

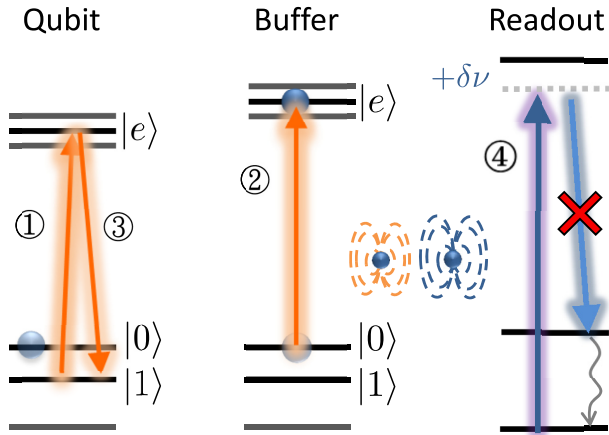


FIG. 2. (Color online) Pulse sequence for reading out the state of one qubit via one buffer ion and the readout ion (note that the buffer is just the closest qubit ion). In the instance shown the qubit is in the  $|0\rangle$  state, and the first pulse, (1), resonant with the  $|1\rangle \rightarrow |e\rangle$  qubit transition, does not excite it. The buffer ion is now unshifted, and a pulse, (2), resonant with the  $|0\rangle \rightarrow |e\rangle$  buffer transition will cause an excitation of the buffer ion. At this stage, the qubit ion is coherently returned to the ground state by pulse (3), such that it spends a minimum amount of time in the excited state. Finally, the readout ion is continuously excited and light is detected, (4). In the current example, the readout ion was shifted due to an excited buffer ion, and there is no fluorescence. However, if the qubit were originally in the  $|1\rangle$  state, pulse (2) would be off resonant, and the buffer would not get excited, and thus the readout ion would instead fluoresce.

a mode volume of a few wavelengths cubed [20], a Purcell factor higher than  $10^4$  can be achieved. Taking into account the decay branching ratios, we then obtain an effective readout ion lifetime of about 200 ns, which can thus be cycled many times during the duration of the qubit excitation, as  $T_{1,\text{Eu}} = 1.9$  ms. The collection efficiency of a typical fluorescence detection setup may be about 1%. However, in a cavity with a high Purcell factor, almost all light will be spontaneously emitted into the same spatial mode. This can yield collection efficiencies in excess of 90%, and including other factors like detector quantum efficiency can allow a total detection efficiency to go up to 10%. Scenarios with different collection efficiencies have been simulated using a Monte Carlo method for both qubit starting states,  $|0\rangle$  and  $|1\rangle$ , as shown in Fig. 3. The simulations are purely statistical in nature; that is, they do not account for any coherent dynamics, only state occupations, updated at short time steps based on decay probabilities. The blue histograms show the number of collected photons when the readout ion is unshifted (qubit in state  $|1\rangle$  before the excitation pulse), and the red ones show the number of collected photons when it is shifted (qubit in state  $|0\rangle$  before the excitation pulse). The best discrimination between the two states is achieved for different photon collection times depending on the total collection efficiency and background light level. For instance, for 1% collection efficiency, a photon collection time of  $0.15T_{1,\text{Eu}}$  was found to be optimal, with the probability to determine the correct state reaching approximately 93%. The largest source of error here is spontaneous decay of the qubit

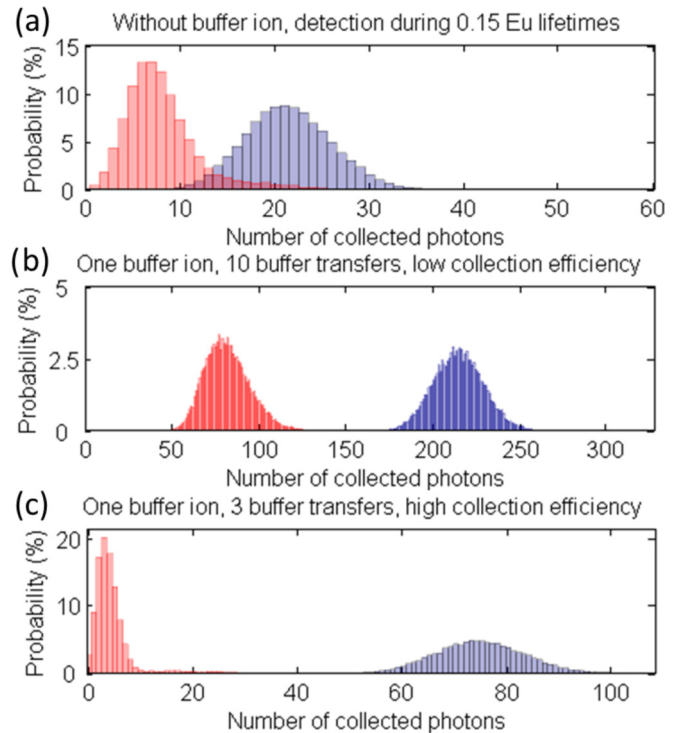


FIG. 3. (Color online) Histograms of simulated photon statistics for detection of a single Nd ion in a cavity. In (a), the readout ion Nd is directly controlled by the qubit ion. In (b) and (c) the cumulative statistics is shown from 10 and 3 repeated readouts, respectively, using one buffer step. The vertical axis shows the probability of receiving  $n$  photons during the optimal photon collection time, and the corresponding probabilities of correctly distinguishing the states are (a) 93%, (b) 99.7%, and (c) 99.85%. For (b) and (c), detection efficiencies of 1% and 10%, respectively, have been used, which also makes it possible to obtain good distinguishability with fewer buffer transfers in (c).

ion due to the finite lifetime of Eu. For a 10% collection efficiency, the optimal collection time was instead  $0.025T_{1,\text{Eu}}$ .

The readout protocol can be improved significantly by introducing a buffer ion between the qubit ion and the readout ion, as shown in Fig. 2. For the discussion we use the same ion species for the buffer as for the qubit, but another species could potentially be used with some advantages. Now, two mutually interacting qubit ions are used, where one of them, the buffer ion, can control the readout ion. Selective excitation of different qubit ions and the buffer ion can generally be carried out as different ions have different resonance frequencies; that is, they sit on different parts of the inhomogeneous profile. First, one pulse is used to state selectively excite the qubit ion; then a second pulse is used to selectively excite the buffer ion, conditioned on the qubit ion not being excited. A third pulse then coherently deexcites the qubit ion back to the ground state if it was excited during the earlier stage (i.e., the third pulse is effectively the inverse of the first pulse). After this selective excitation the buffer ion state is read out as described above, and the number of photons from the readout ion during the  $0.15T_{1,\text{Eu}}$  detection time is counted. This pulse sequence is illustrated in Fig. 2.

After one detection event, the buffer ion can be reinitialized through optical pumping. The qubit ion is still in its original state, and the same pulse sequence can be applied again to make another fluorescence measurement, yielding further information about the same qubit ion state. This process can be repeated several times, such that the total effective number of detected photons that depends on the qubit state can be increased substantially. The optimal number of times to repeat this buffering sequence depends on the detection efficiency and the background light level of the particular setup. Figures 3(b) and 3(c) show two different setups with 1% and 10% detection efficiency, respectively, that both can reach a probability of readout of the correct qubit state of about 99.7%–99.9%. For the gate fidelity simulations described in the next section we will assume a representative readout error of  $2 \times 10^{-3}$ . We note that roughly the same state distinguishability can be reached for both cases, showing that the scheme is robust against such experimental parameters but that a larger number of buffer transfers is needed for lower detection efficiency. The final error is given mostly by the amount of time the qubit ion spends in the excited state, which cannot be reduced lower than the time it takes to do a state transfer on the buffer ion (see Sec. IV for more details). In principle, further buffer stages could be concatenated for an exponentially decreasing error probability; however, the buffer state transfer time of 400 ns relative to the Eu excited state lifetime makes protocols with more than one buffer stage unrewarding for Eu in particular (but could still be useful for other setups).

#### IV. CNOT GATE FIDELITY

A full CNOT gate experiment will include the following steps:

- (1) Initialization
- (2)  $\pi/2$  pulse, between  $|0\rangle$  and  $|1\rangle$ , on the control qubit
- (3)  $\pi$  pulse,  $|0\rangle \rightarrow |e\rangle$ , on the control qubit
- (4) NOT on the target qubit
- (5)  $\pi$  pulse reversing the excitation in step 3
- (6) Readout

The different steps in the list above will now be described in detail, including assumptions and expected errors for each step. The total CNOT error obtained in the end will include the error from all steps, with care taken to model the different nature of the errors. We use a discrete time model in which each step is represented using operator sum notation (for details see, e.g., Nielsen and Chuang [26]). For example, any transfer pulse will cause both bit- and phase-flip errors, represented by bit- and phase-flip channels, respectively, while any time spent in the excited state will be subject to lifetime decay, modeled as an amplitude-damping channel.

(1) *Initialization.* The initialization step starts with finding a suitable chain of ions that can function as buffer and qubits and can be described in four main steps (for an overview picture of the different parts of the chain, also see Fig. 1): (i) A readout ion is found by scanning a laser tuned to the readout ion transition in frequency until fluorescence is observed. (ii) The readout laser is kept on, and another laser is now tuned to the qubit ion transition in a similar way. The qubit ions are then excited using  $\pi$  pulses to invert the population, and each frequency channel in the inhomogeneous width of the qubit

ions is consecutively scanned through until the fluorescence from the readout stops. This means that an ion sufficiently close to the readout ion to shift it in frequency has now been excited. This will be the buffer ion (compare with Fig. 2). (iii) Still keeping the readout laser on, the inhomogeneous width of the qubit ions is scanned from the start again, repeating the excitation procedure described in the previous step. For each frequency channel throughout the new scan, a  $\pi$  pulse is applied on that frequency but is now followed by a  $\pi$  pulse also exciting the buffer ion, while we monitor when the readout ion resumes fluorescing. This indicates that the frequency of an ion that can control the buffer ion, shifting it out of resonance, has been identified. This will be the first qubit ion. (iv) Repeat the previous step one more time, such that two qubit ions that are both in the vicinity of the buffer ion are found. They will most likely also be sufficiently close to each other, but if they are not and longer chains of ions are desired, the step is instead extended to find ions that shift the previous qubit ion, thus stopping it from controlling the buffer ion. This process can be nested as many layers away from the readout ion as it takes, with the overhead cost of only one extra pulse per layer away.

After a sufficient chain of controlling ions has been established, the qubit ions should be initialized to the  $|0\rangle$  state, which can be done by means of optical pumping to an auxiliary state followed by a frequency-selective state transfer back in a manner similar to that of protocols used previously in the ensemble approach [10]. The error during the initialization step is therefore assumed to be equal to the error of the final transfer pulse (a sech; see Sec. II for details); that is, the starting state is considered to be a mixed state with a probability of being in the wrong level of  $4 \times 10^{-4}$  for each qubit.

(2)  *$\pi/2$  pulse between  $|0\rangle$  and  $|1\rangle$  on the control qubit.* Transitions between the nuclear-spin states cannot be directly driven by a single optical laser field. However, two simultaneous laser fields, where the difference frequency matches the nuclear-spin levels, can accomplish arbitrary single-qubit gates using a dark-state technique, as demonstrated in Ref. [10]. These pulses have the same duration as the transfer pulses (defined in Sec. II) and thus essentially have the same error. For an arbitrary gate two successive such bi-chromatic pulses are needed, which will yield phase- and bit-flip errors twice as large as those of a transfer pulse, i.e.,  $8 \times 10^{-4}$  on the control qubit.

(3)  *$\pi$  pulse,  $|0\rangle \rightarrow |e\rangle$ , on control qubit.* This step is a straightforward sech pulse, with phase- and bit-flip errors both considered to be  $4 \times 10^{-4}$  for the control qubit.

(4) *NOT on target qubit.* Although the target qubit operation is conditioned on the control ion not causing a frequency shift, this step is essentially just a  $\pi$  pulse on the nuclear-spin levels, i.e., a single-qubit gate, making an error on the target qubit equal to  $8 \times 10^{-4}$ . In addition, while waiting for the gate to be performed, the control qubit spends two pulse durations in the excited state, which gives a decay probability due to limited lifetime of  $1 - e^{-0.8\mu\text{s}/1.9\text{ms}} \approx 4 \times 10^{-4}$ .

(5)  *$\pi$  pulse reversing the excitation in step 3.* This step has the same operation and errors as the step 3 excitation.

(6) *Readout.* For the purpose of finding the achievable CNOT fidelity we use the scheme with one buffer ion, as described above, using a readout error of  $2 \times 10^{-3}$  that we obtained

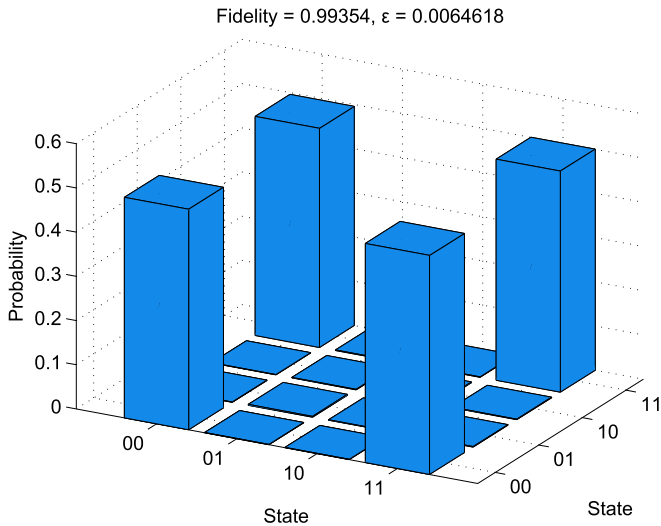


FIG. 4. (Color online) The (real) elements of the density matrix of a prepared Bell state, including all error sources as described in the text. The total fidelity is 99.4% without readout and 99.1% with readout.

earlier (Sec. III). Note that this error is asymmetrical; that is, it represents the probability that a  $|0\rangle$  is counted as a  $|1\rangle$ . The reverse error is usually much smaller because the main error decays from the excited state, and state  $|1\rangle$  is never excited.

*Final experiment fidelity.* The effects of all operations described above are calculated from actions applied to a starting density matrix. In the end when all steps have been taken into account, but before the readout, the system will be in a final density matrix  $\rho_f$ . We can then compute the fidelity of the state as  $F = \langle \psi_{\max} | \rho_f | \psi_{\max} \rangle$ , where  $\psi_{\max}$  is the state we aim to create, such as a maximally entangled Bell state. Without the readout step, the total error  $\varepsilon = 1 - F$  is found to be  $\sim 6 \times 10^{-3}$ . The readout is included by allowing the calculated density matrix to be sampled as it would during a real readout sequence, with projections to the four possible two-qubit states. A quantum-state-tomography sequence was then simulated using 15 different observables in 9 different measurement settings (see, e.g., [27]). This gives a recreated density matrix (shown in Fig. 4) that can be used to obtain the fidelity, including the readout stage, and we find the total error to be  $\sim 9 \times 10^{-3}$ . This means that both the coherent operations and the readout process contribute significantly to the overall fidelity, which emphasizes the need for using the proposed readout buffer stage.

Note that while an effort has been made to include most systematic error sources, a real experiment will also include random projection noise caused by a limited number of experimental count cycles, but that has not been included here. In practice, this error will be limited by the total duration of the full protocol, and since gate operations can be made in submicroseconds, the largest time is consumed by the readout stage. However, the fluorescence detection itself is not the main culprit, as a buffer stage with 10 repetitions, each one with a photon collection time of  $0.15T_{1,\text{Eu}}$  or better, will last a maximum of 3 ms, which is comparable to other single-ion detection rates. Instead, the main time consumption arises

from the reinitialization of the buffer step that has to be done between each repetition cycle. If simple optical pumping via the long-lived excited state is used to reset the buffer state, then several lifetimes of Eu has to be used to reset it with good fidelity, which is a few tens of milliseconds per repetition. To circumvent this, a quenching mechanism can be used by means of stimulating the transition from the excited state down to another Stark level, which then decays very fast to the ground state by nonradiative processes.

## V. SCALABILITY

The previous section detailed the specific case of a two-qubit gate, where the errors were included in a careful manner in the total density matrix describing the system. This approach is difficult to extend to larger qubit systems, as the size of the Hilbert space scales exponentially with the number of qubits. In this section, we will attempt to give some figures for the scaling of larger qubit states by simpler considerations based on the values of the CNOT gate obtained in the previous section. We will focus on the expected fidelity of an  $n$ -qubit Greenberger-Horne-Zeilinger (GHZ) state of the form  $|\Psi\rangle = |0 \cdots 0\rangle + |1 \cdots 1\rangle$ , which is a simple yet useful type of entangled state. The expected fidelity of this state can be fairly straightforwardly calculated by realizing that it is created by  $n - 1$  successive CNOT gates. Moreover, this fidelity will be the same both for the case of only nearest-neighbor interactions and for the case where each ion can control each of the other ions. This result is shown in Fig. 5, both with and without readout. One limitation of the prediction is that while the creation of the GHZ state allows situations where only nearest-neighbor interactions are possible, the readout step is calculated with the assumption that each ion can control a buffer ion directly without additional swap operations. As discussed earlier in Sec. II, this is expected to be a reasonable case for at least up to five qubits for a doping concentration of 4%. The obtained fidelities indicate that the single-instance

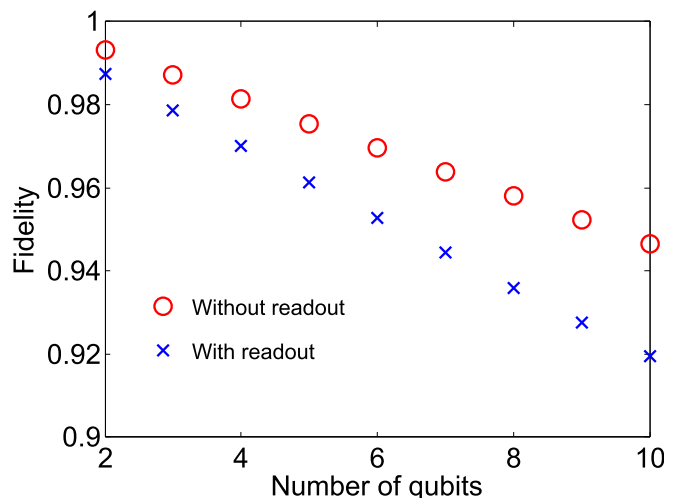


FIG. 5. (Color online) Predicted fidelity of  $n$ -qubit GHZ states with and without readout. The fidelity includes pulses for tomography but assumes that all ions can interact with each other, which is reasonable at least up to five qubits with 4% doping concentration.

rare-earth quantum computer schemes can be comparable to those of other multiqubit schemes, such as trapped ions [2] or superconducting qubits [28].

## VI. CONCLUSIONS

We have presented and described how to realize a readout scheme for detecting quantum states of single ions inside a crystal host. The scheme is based on having a buffer ion, onto which the state of the qubit ions can be repeatedly mapped. This buffer ion is within dipole-dipole interaction range of a readout ion, and the state of the buffer ion can control the excitation frequency of the readout ion. This will enable or disable excitation of the readout ion, and the state can thus be detected by cavity-enhanced fluorescence. Several buffer stages can, in principle, be concatenated to yield very long effective detection times, such that readout errors can be reduced by more than one order of magnitude and reach  $\varepsilon = 10^{-3}$  for a wide variety of collection efficiencies and background levels. We then used this result together with

known error sources to obtain expected fidelities for a CNOT gate of above 99% and for larger GHZ states remaining above 92% for up to ten qubits. One of the limitations of our assumptions is presently that the expected increase in performance for qubit rotations when switching from Pr to Eu has not been fully experimentally verified as of yet. Our results indicate that rare-earth quantum computing can be feasible in the single-instance regime.

## ACKNOWLEDGMENTS

The authors acknowledge useful discussions with D. Hunger. This work was supported by the Swedish Research Council, the Knut and Alice Wallenberg Foundation, and the Crafoord Foundation. The research leading to these results also received funding from the People Programme (Marie Curie Actions) of the European Union's Seventh Framework Programme FP7 (2007-2013) under REA Grant Agreement No. 287252 (CIPRIS), Lund Laser Center (LLC), and the Nanometer Structure Consortium at Lund University (nmC@LU).

- 
- [1] H. Häffner, W. Hänsel, C. F. Roos, J. Benhelm, D. Chek-al-kar, M. Chwalla, T. Körber, U. D. Rapol, M. Riebe, P. O. Schmidt, C. Becher, O. Gühne, W. Dür, and R. Blatt, *Nature (London)* **438**, 643 (2005).
- [2] T. Monz, P. Schindler, J. T. Barreiro, M. Chwalla, D. Nigg, W. A. Coish, M. Harlander, W. Hänsel, M. Hennrich, and R. Blatt, *Phys. Rev. Lett.* **106**, 130506 (2011).
- [3] X. -C. Yao, T. -X. Wang, P. Xu, H. Lu, G. -S. Pan, X. -H. Bao, C. -Z. Peng, C. -Y. Lu, Y. -A. Chen, and J. -W. Pan, *Nat. Photonics* **6**, 225 (2012).
- [4] M. H. Devoret and R. J. Schoelkopf, *Science* **339**, 1169 (2013).
- [5] J. Wrachtrup and F. Jelezko, *J. Phys. Condens. Matter* **18**, S807 (2006).
- [6] H. Riedmatten, M. Afzelius, M. U. Staudt, C. Simon, and N. Gisin, *Nature (London)* **456**, 773 (2008).
- [7] M. Afzelius, I. Usmani, A. Amari, B. Lauritzen, A. Walther, C. Simon, N. Sangouard, J. Minár, H. de Riedmatten, N. Gisin, and S. Kröll, *Phys. Rev. Lett.* **104**, 040503 (2010).
- [8] M. P. Hedges, J. J. Longdell, Y. Li, and M. J. Sellars, *Nature (London)* **465**, 1052 (2010).
- [9] E. Fraval, M. J. Sellars, and J. J. Longdell, *Phys. Rev. Lett.* **95**, 030506 (2005).
- [10] L. Rippe, B. Julsgaard, A. Walther, Y. Ying, and S. Kröll, *Phys. Rev. A* **77**, 022307 (2008).
- [11] J. H. Wesenberg, K. Mølmer, L. Rippe, and S. Kröll, *Phys. Rev. A* **75**, 012304 (2007).
- [12] R. Kolesov, K. Xia, R. Reuter, R. Stöhr, A. Zappe, J. Meijer, P. Hemmer, and J. Wrachtrup, *Nat. Commun.* **3**, 1029 (2012).
- [13] T. Utikal, E. Eichhammer, L. Petersen, A. Renn, S. Götzinger, and V. Sandoghdar, *Nat. Commun.* **5**, 3627 (2014).
- [14] D. B. Hume, T. Rosenband, and D. J. Wineland, *Phys. Rev. Lett.* **99**, 120502 (2007).
- [15] D. Kielpinski, C. Monroe, and D. Wineland, *Nature (London)* **417**, 709 (2002).
- [16] M. Zhong, M. P. Hedges, R. L. Ahlefeldt, J. G. Bartholomew, S. E. Beavan, S. M. Wittig, J. J. Longdell, and M. J. Sellars, *Nature (London)* **517**, 177 (2015).
- [17] A. Walther, B. Julsgaard, L. Rippe, Y. Ying, S. Kröll, R. Fisher, and S. Glaser, *Phys. Scr. T* **137**, 014009 (2009).
- [18] Y. Yan, J. Karlsson, L. Rippe, A. Walther, D. Serrano, D. Lindgren, M. -E. Pistol, S. Kröll, P. Goldner, L. Zheng, and J. Xu, *Phys. Rev. B* **87**, 184205 (2013).
- [19] R. Kolesov, K. Xia, R. Reuter, M. Jamali, R. Stöhr, T. Inal, P. Siyushev, and J. Wrachtrup, *Phys. Rev. Lett.* **111**, 120502 (2013).
- [20] H. Kaupp, C. Deutsch, H. -C. Chang, J. Reichel, T. W. Hänsel, and D. Hunger, *Phys. Rev. A* **88**, 053812 (2013).
- [21] F. Könz, Y. Sun, C. W. Thiel, R. L. Cone, R. W. Equall, R. L. Hutcheson, and R. M. Macfarlane, *Phys. Rev. B* **68**, 085109 (2003).
- [22] I. Roos and K. Mølmer, *Phys. Rev. A* **69**, 022321 (2004).
- [23] R. W. Equall, Y. Sun, R. L. Cone, and R. M. Macfarlane, *Phys. Rev. Lett.* **72**, 2179 (1994).
- [24] A. N. Nilsson, L. Rippe, A. Walther, and S. Kröll (unpublished).
- [25] N. Ohlsson, R. K. Mohan, and S. Kröll, *Opt. Commun.* **201**, 71 (2002).
- [26] M. A. Nielsen and I. L. Chuang, *Quantum Computation and Quantum Information* (Cambridge University Press, Cambridge, UK, 2000), Chap. 8.
- [27] C. F. Roos, G. P. T. Lancaster, M. Riebe, H. Häffner, W. Haensel, S. Gulde, C. Becher, J. Eschner, F. Schmidt-Kaler, and R. Blatt, *Phys. Rev. Lett.* **92**, 220402 (2004); [arXiv:quant-ph/0307210](https://arxiv.org/abs/quant-ph/0307210).
- [28] R. Barends *et al.*, *Nature (London)* **508**, 500 (2014).